Impact of model free parameters and sea-level rise uncertainties on 20-years shoreline hindcast: the case of Truc Vert beach (SW France)

Maurizio d'Anna, Déborah Idier, Bruno Castelle, Gonéri Le Cozannet, Jeremy Rohmer, Arthur Robinet

Impact of model free parameters and sea-level rise uncertainties on 20-years shoreline hindcast: the case of Truc Vert beach (SW France)

Maurizio D'Anna[1,2], Déborah Idier[1], Bruno Castelle[2], Gonéri Le Cozannet[1], Jeremy Rohmer[1], Arthur Robinet[1]

[1] BRGM (French Geological Survey), Orléans, France.

[2] UMR EPOC, CNRS, Université de Bordeaux, Pessac, France.

Correspondence

Maurizio D'Anna, Department of Risk and Prevention, R3C, BRGM, 3 Av. Guillemin, Orléans, France, 45000.

Email: m.danna@brgm.fr

Funding information

BRGM (French Geological Survey);

Make Our Planet Great Again (MOPGA)

Published version

The final version of this article was published by Earth Surface Processes and Landforms, Wiley:

D'Anna M., Idier D., Castelle B., Le Cozannet G., Rohmer J., and Robinet A. 2020. Impact of model free parameters and sea-level rise uncertainties on 20-years shoreline hindcast: the case of Truc Vert beach (SW France). ESPL, 45(8), 1895-1907. https://doi.org/10.1002/esp.4854

Abstract

Shoreline change is driven by various complex processes interacting at a large range of temporal and spatial scales, making shoreline reconstructions and predictions challenging and uncertain. Despite recent progress in addressing uncertainties related to the physics of sea-level rise, very little effort is made towards understanding and reducing the uncertainties related to wave-driven shoreline response. To fill this gap, the uncertainties associated with the long-term modelling of shoreline change are analysed at a high-energy cross-shore transport dominated site. Using the state-of-the-art LX-Shore shoreline change model, we produce a probabilistic shoreline reconstruction, based on 3000 simulations over the past 20 years at Truc Vert beach, southwest France, whereby sea-level rise rate, depth of closure and three model free parameters are considered uncertain variables. We further address the relative impact of each source of uncertainty on the model results performing a Global Sensitivity Analysis. This analysis shows that the shoreline changes are mainly sensitive to the three parameters of the wave-driven model, but also that the sensitivity to each of these parameters is strongly modulated seasonally and interannually, in relation with wave energy variability, and depends on the time scale of interest. These results have strong implications on the model skill sensitivity to the calibration period as well as for the predictive skill of the model in a context of future climate change affecting wave climate and extremes.

KEYWORDS

Sea-level rise, shoreline modelling, Truc Vert, France, global sensitivity analysis (GSA), uncertainties, erosion.

1. INTRODUCTION

Most of the coastlines around the world are constantly evolving features. Recent studies have shown that currently shoreline retreat dominates globally, mostly because of the anthropologic pressure (Mentaschi, Vousdoukas, Pekel, Voukouvalas, & Feyen, 2018), exposing coastal settlements to hazard. This is a significant concern considering the expected population growth in low-lying coastal zones, especially in developing countries (Neumann, Vafeidis, Zimmermann, & Nicholls, 2015; Wong et al., 2014). Sandy beaches cover about 31% of ice-sheet free coasts worldwide (Luijendijk et al., 2018), and are particularly important features for coastal communities around the globe (Ghermandi & Nunes, 2013), providing economical and recreational value as well as being an efficient buffer against storm waves. However between 24% and 70% of sandy coasts are estimated to be already under chronic erosion (Bird, 1985; Luijendijk et al., 2018).

In a context of climate change and sea-level rise, knowing the future shoreline behaviour is a critical concern for coastal management and adaptation planning (Hinkel et al., 2019; Toimil, Diaz-Simal, Losada, & Camus 2018; Wainwright et al., 2015). Wave-dominated sandy beaches are highly dynamic and evolve permanently in response to changes in wave regimes (Wright & Short, 1984). The processes controlling shoreline change are complex and interact at different temporal and spatial scale, making pluri-decadal simulations challenging and hardly reliable (Ranasinghe, 2020; Vitousek, Barnard, & Limber 2017). In addition, modelled shoreline change inherit uncertainties of driving processes (e.g. sea-level rise) as well as uncertainties related to the modelling assumptions.

Most studies addressing uncertainties of shoreline behaviour at decadal timescales rely on data-driven approaches, based on extrapolated observations or empirical

models calibrated with measured data (Allenbach et al., 2015; Casas-Prat, McInnes, Hemer, & Sierra 2016; Le Cozannet et al., 2016, 2019; Ranasinghe, 2020; Toimil, Losada, Camus, & Diaz-Simal, 2017). Reduced-complexity models (RCMs) have been proposed as a way forward to increase the reliability of long-term shoreline modelling (Castelle et al., 2014; Davidson, Splinter, &, Turner, 2013; Hallin, Larson, & Hanson, 2019; Robinet, Idier, Castelle, & Marieu, 2018; Splinter, Turner, Davidson, Bernard, & Castelle, 2014; Vitousek, Barnard, Limber, Erikson, & Cole, 2017; Yates, Guza, & O'Reilly, 2009). RCMs typically consider general principles, such as semi-empirical and behaviour rules. On cross-shore transport dominated sites, RCMs that address shoreline change from the timescales of hours (storm) to years and decades are often based on the dis-equilibrium concept (Wright & Short, 1984), whereby the rate of shoreline change is governed by the difference between present and equilibrium conditions. These equilibrium conditions can be defined in terms of shoreline position (Yates et al., 2009) or wave history (Davidson et al., 2013). This generation of RCMs has been applied successfully at many sites where longshore processes have little influence on shoreline variability (e.g. Castelle et al., 2014; Dodet et al., 2019; Ludka, Guza, O'Reilly, & Yates, 2015; Lemos et al., 2018; Montaño et al. (2020); Robinet, Castelle, Idier, Harley & Splinter, 2020; Splinter et al., 2014). However, these RCMs rely heavily on a data-driven approach to search for the best free parameters. Duration and quality of shoreline data, for which minimum requirements have been subject to debate (Splinter, Turner, & Davidson, 2013), are important with model skill increasing with increasing calibration data period and frequency (Splinter et al., 2013). More recently it has been shown that a subtle changes in the seasonality of storms can have a profound impact on the shoreline mode of variability, for instance from a seasonally-dominated mode (annual cycle) to a storm-dominated (~monthly) mode at Narrabeen,

SE Australia (Splinter, Turner, Reinhardt, & Ruessink, 2017). This shows that changes in the intra-annual and interannual distribution of wave energy, resulting from natural modes of climate variability or from climate change, is critical to the shoreline mode of response and, in turn, the free parameters of RCMs, although this is still poorly understood.

In this contribution, we analyse the effect of uncertainties in sea-level rise (SLR) rate, depth of closure (DoC) and shoreline model free parameters on a 20-year shoreline hindcast using a state-of-the-art shoreline change model LX-Shore (Robinet et al., 2018) and performing a variance-based Global Sensitivity Analysis (see Saltelli et al., 2008). This approach is applied to the high-energy, cross-shore transport dominated sandy beach of Truc Vert, SW France. The variance-based Global Sensitivity Analysis (GSA) allows assessing the respective contributions of uncertain physical inputs and empirical parameters to the uncertainty in the shoreline hindcast and analysing their variation in time in response to changes in the inter- and intra-annual distribution of wave energy. The paper proceeds as follows. Section 2 provides a description of Truc Vert beach, the data and the modelling setup used for this study, as well as the GSA methodology. Section 3 describes the design of the probability distributions for each uncertain input variable. In Section 4 we present the application of the methodology to Truc Vert beach showing the probabilistic modelling results and the corresponding evolution of the sensitivity indices for all variables. Finally, in Section 5 we discuss the implications from the perspectives of model calibration and potential forecast application in the frame of a changing climate, as well as the limitations of the present work.

2. SITE, DATA AND METHOD

2.1 Study Area

Truc Vert is an open macro-tidal and wave-dominated sandy beach located in SW France, backed by a large and high dune (Figure 1a,b). The largest astronomical tide range exceeds 4.9 m, and tide-driven currents are mostly negligible compared to wave-driven currents. The wave climate is energetic and strongly seasonally modulated with a monthly-averaged significant wave height Hs ranging from 1.1m in July with a dominant W-NW direction to 2.4m in January with a dominant W direction (Castelle, Bujan, Ferreira, & Dodet, 2017). Winter wave energy is strongly variable interannually (Castelle et al., 2018; Charles et al., 2012; Robinet et al., 2016) owing to large-scale climate patterns of atmospheric variability in the north Atlantic, primarily the West Europe Anomaly and to a lesser extent the North Atlantic Oscillation (Castelle, Dodet, Masselink, & Scott, 2017). The sediment consists of well-mixed fine to medium sand with a mean grain size of about 0.35–0.40mm (Gallagher, MacMahan, Reniers, Brown, & Thornton, 2011). The beach morphology is strongly variable alongshore, typically double barred with the inner intertidal sandbar classified as transverse bar and rip (Sénéchal et al., 2009), and the outer bar as crescentic (Castelle, Bonneton, Dupuis, & Sénéchal, 2007). On the long term, this stretch of coast has been reasonably stable (Castelle, Dodet, Masselink, & Scott, 2018), although the strongly interannual variable winter energy of waves can result in extreme winters causing severe beach and dune erosion (Castelle et al., 2015; Masselink et al., 2016). Overall, the shoreline evolution is mainly dominated by cross-shore processes with strong seasonal and interannual variability (Castelle et al., 2014; Robinet et al., 2016, 2018).

Figure 1 (a) Location of Truc Vert beach (green) and of the wave hindcast grid point co-located with CANDHIS in situ wave buoy (red); (b) picture of Truc Vert beach landscape (Photo from V. Marieu); and (c) alongshore-averaged beach-dune profile from the combination of topo-bathymetry (2008) and UAV-photogrammetry digital elevation model (2018)

2.2 Shoreline, waves and mean sea level data

2.2.1 Shoreline and topo-bathymetry

Monthly or bimonthly sampled topographic DGPS surveys have been performed at spring low tide from April 2005 to December 2017 with a 1-year gap between 2008 and 2009. The alongshore coverage of the surveys increased over the years: from 350m to 750m in 2005-2008, from 750m to 1200m in 2008-2012 and from 1200m to 1900m starting from 2012 to present. The shoreline proxy used here is the mean high water level (+1.5m above the local mean sea level), in agreement with previous studies at Truc Vert (Castelle et al., 2014), as it is the shoreline proxy that gives the best correlation with the total beach-dune volume (Robinet et al., 2016). In order to compute the main characteristics of the active profile at Truc Vert (Figure 1c), which are critical in addressing the influence of SLR on shoreline response, we used a 2-m resolution topo-bathymetry collected in 2008 at Truc Vert (Parisot et al., 2009). The data cover the nearshore area from the elevation of -10m to approximately +2m IGN69

(approximately mean sea level). In addition, we used recent high-resolution digital elevation model inferred from UAV-photogrammetry between October 2017 and October 2018 covering 4km of beach-dune system (Laporte-Fauret et al., 2019).

2.2.2 Wave Climate

A 24-year of hourly wave hindcast (1994-2018) was gathered from the NORGAS-UG regional model (Michaud et al., 2016) at the grid point co-located with the in situ CANDHIS wave buoy moored in ~50m depth offshore of Truc Vert beach (Figure 1a). The NORGAS-UG model covers the Atlantic French coastal area using an unstructured mesh with resolution ranging from 10km offshore to 200m nearshore. Figure 2 shows the time series of offshore wave conditions at Truc Vert over 1994-2018 highlighting a strong seasonal and interannual signal with prevailing W-NW incidence.

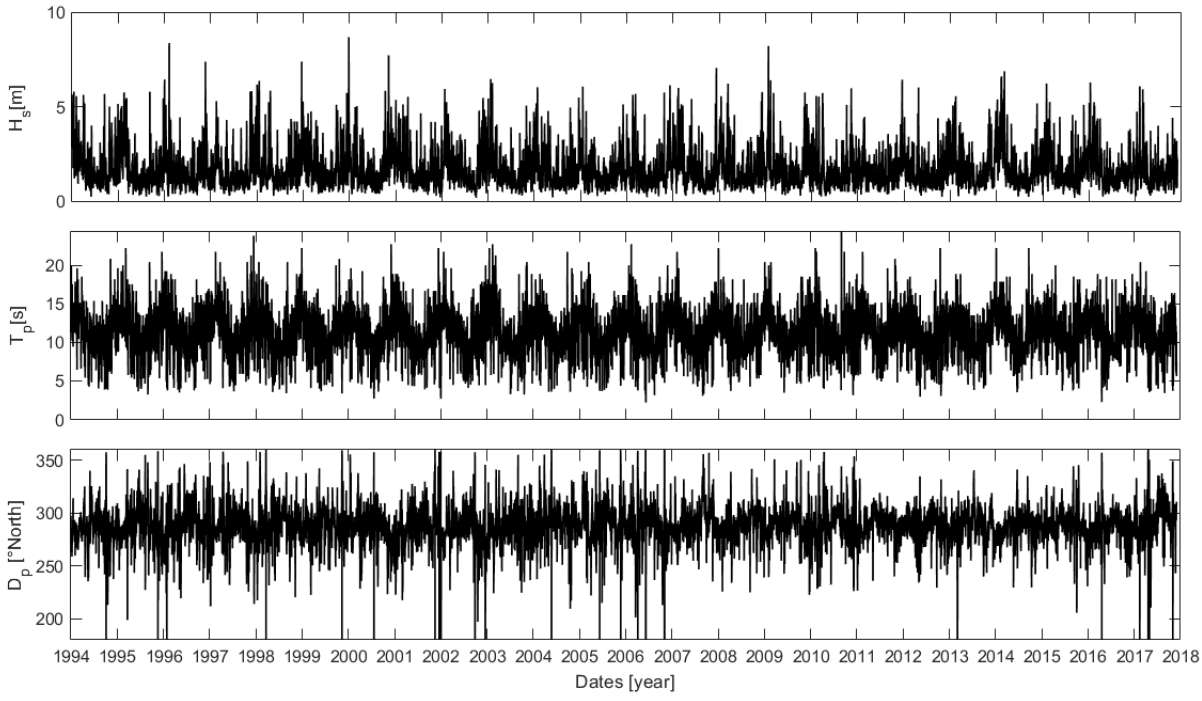

Figure 2 NORGAS-UG wave hindcast time series from 1994 to 2018 at (44°39'9'' N; -1°26'48'' W) offshore of Truc Vert beach (see Figure 1a): (a) significant wave height; (b) peak wave period; and (c) peak wave direction expressed in Nautical convention

2.2.3 Mean Sea Level and Vertical Land Motion

The absolute mean sea level time series at the Bay of Biscay was reconstructed between 1998 and 2017 using a Bayesian statistical approach (Rohmer & Le Cozannet, 2019). During the past 20 years, the mean sea level rose at a roughly constant rate of 2.1(± 0.1)mm/year. To estimate SLR relative to the land, the contribution of local vertical land motion (VLM) needed also to be estimated. For this purpose, we used the near Cap-Ferret permanent GNSS station from the SONEL database (Santamaría-Gómez et al., 2017), which provides observations until August 2016, when the station was decommissioned. It is unsure that the pointwise information of the permanent GNSS station located at Cap-Ferret is representative of the nearby area, and this belongs to residual uncertainties. The data show a subsidence rate of 1.21 (± 0.57)mm/year, resulting in a relative mean sea level rising at a roughly constant rate of 3.31 (±0.67)mm/year over the period of interest (Figure 3).

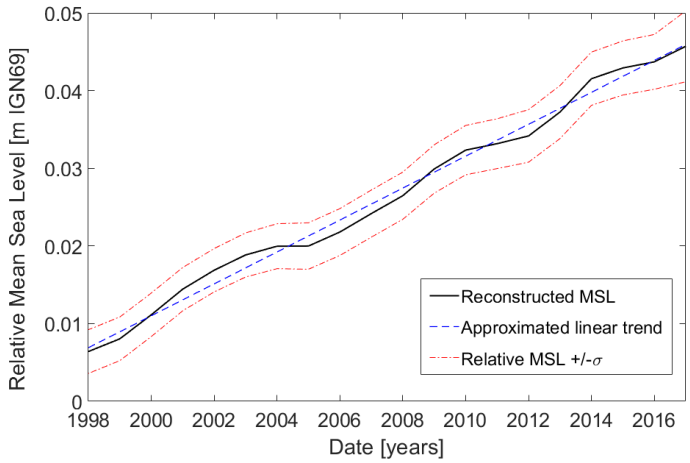

Figure 3 Relative Mean Sea Level time series relative to Cap-Ferret land elevation (m NGF IGN69), with linear approximations over 1998-2018

2.3 Shoreline evolution model

In this study we used the LX-Shore shoreline evolution model (Robinet et al., 2018, 2020). In LX-Shore, shoreline change is primarily driven by the gradients in total longshore sediment transport and by the cross-shore transport owing to variability in incident wave energy. Herein, LX-Shore is used in a simple configuration with (i) the longshore sand transport module switched off given that Truc Vert is known to be a cross-shore transport dominated site (Castelle et al., 2014; Splinter et al., 2014), and (ii) breaking wave conditions directly computed from offshore wave conditions using the Larson, Hogan, & Hanson (2010) formula given that offshore bathymetric iso-contours are essentially shore parallel. In addition to the model presented in Robinet et al. (2018) we include a module accounting for shoreline retreat through the model of Bruun (1962). The study period covers 20 years (from January 1998 to December 2017). In what follows, we further describe the 2 main modules used in the present study, i.e. the cross-shore module and the sea-level rise module.

2.3.1 Cross-Shore module

The LX-Shore cross-shore module is an adaptation of the ShoreFor empirical model described in Davidson et al. (2013) and Splinter et al. (2014), which defines the shoreline displacement as a function of the nearshore wave power and a disequilibrium state of the beach. In this type of approach, the cross-shore rate of shoreline change (dY/dt; m/s) is calculated as:

$$\frac{dY}{dt} = c(F^{+} + rF^{-}) + b \qquad (1)$$

where c ($m^{1.5}s^{-1}W^{-0.5}$) is the response rate parameter, and b (m/s) a linear component that accounts for longer-term processes that are not explicitly included in the model.

The hydrodynamic forcing (F) combines the effects of the wave power available to move sediment and the disequilibrium condition as follows:

$$F = \mathrm{P}^{0.5}\frac{\Delta\Omega(\Phi)}{\sigma_{\Delta\Omega}} \quad (2)$$

where P (W) is the incident wave power at breaking, $\Delta\Omega$ quantifies the disequilibrium state as a function of the previous wave conditions, and $\sigma_{\Delta\Omega}$ is the standard deviation of $\Delta\Omega$. In ShoreFor the disequilibrium beach state ($\Delta\Omega$) at each time step is expressed as the difference between an equilibrium dimensionless fall velocity (Ω_{eq}) and the dimensionless fall velocity at breaking (Ω_b), where Ω_{eq} is defined as a function of the previous wave conditions, sediment size and a site-specific beach memory parameter (Φ) expressed in days:

$$\Delta\Omega(\Phi) = \Omega_{eq}(\Phi) - \Omega_b \quad (3)$$

$$\Omega_{eq}(\Phi) = \Sigma_{i=1}^{2\Phi}\,\Omega_{b,i}10^{-i/\Phi}\left[\Sigma_{i=1}^{2\varphi}10^{-i/\Phi}\right]^{-1} \quad (4)$$

$$\Omega_b = \frac{H_{s,b}}{wT_p} \quad (5)$$

where w (m/s) is the fall velocity, $H_{s,b}$ (m) the significant wave height at breaking and T_p (s) the peak wave period, and i the number of days prior to simulated present time. Based on current disequilibrium state $\Delta\Omega(t)$, a negative $F(t) = F^-$ (Equation 1) denotes an erosive forcing while F^+=0 (Equation 1), and vice versa during constructive conditions ($F(t) > 0$). The LX-Shore adaptation of this model consists in using offshore wave conditions rather than breaking conditions in the formulation of $\Delta\Omega$ (Equation 3):

$$\Delta\Omega(\Phi) = \Omega_{eq}(\Phi) - \Omega_o \qquad (6)$$

$$\Omega_o = \frac{H_{s,o}}{wT_p} \qquad (7)$$

As erosion and accretion are driven by different physical processes, the model accounts for the different shoreline response rate through a scaling factor (*r*) applied on the forcing during erosional events (Equation 1). The *r* factor is not a model free parameter but it is based on the balance between erosion and accretion forcing over the simulated period (Splinter et al., 2014), and it is calculated as:

$$r = \left|\frac{\sum_{i=1}^{N}\langle F^{+}\rangle}{\sum_{i=1}^{N}\langle F^{-}\rangle}\right| \qquad (8)$$

where *N* indicate the total length of the simulated period, || is the absolute value operator, and ⟨ ⟩ represents a numerical operation removing linear trend.

The coefficients c, b and Φ are the three model free parameters which need to be calibrated when the model is applied to a given site. Physically, the parameter *c* ($m^{1.5}s^{-1}W^{-0.5}$) is a measure of the shoreline reactivity to wave forcing at a given time, with the same value for the accretion and erosion phases. *Φ* (days) is a time scale that accounts for the "memory" of the beach to antecedent wave conditions. The parameter *b* (m/s) is a linear trend that accounts for processes that, along with waves and SLR, may drive chronic shoreline change, such as wind driven sediment transport and other slow processes that are not explicitly represented in the model.

2.3.2 Sea-Level Rise module

The contribution of SLR to shoreline change is computed in LX-Shore by means of the Bruun rule (Bruun, 1962). Although the reliability of this rule is still debated (Cooper & Pilkey, 2004; Ranasinghe, Callaghan, & Stive, 2012), it is still largely adopted in practice. The Bruun rule assumes that, on time scales larger than years, the equilibrium beach profile translates while preserving its shape as sea level rises. The consequent shoreline retreat (dY_{SLR}/dt) depends on the increase in sea level and an average slope of the active profile. Here, given the large seasonal and interannual variability of the berm shape and position, and the occasional scarping of the foredune, the dune crest was preferred to define the landward limit of the active profile. Therefore, we assume the active profile extending from the dune crest to the estimated DoC, which is the depth beyond which morphological changes become negligible (Bruun, 1988):

$$\frac{dY_{SLR}}{dt} = \frac{SLR_{rate}}{tan\beta} \qquad (9)$$

where SLR_{rate} is the rate of SLR, and $tan\beta$ is the average slope of the active beach profile vertically delimited by the DoC and the coastal dune height. The DoC was estimated according to Hallermeier (1978) and the resulting $tan\beta$ = 0.0235 was computed from the representative profile in Figure 1c.

2.4 Method (Global Sensitivity Analysis)

When predicting or hindcasting shoreline changes, the uncertainties associated to the input variables cascade through the model producing uncertain results. A way to understand how stochastic input variables affect the uncertainty of the prediction is by conducting a sensitivity analysis. In this study, we use a variance-based GSA (Sobol', 2001; Saltelli et al., 2008). The use of a GSA allows the simultaneous variation of all

the uncertain input parameters, so that their entire range of variability and the range of model output are explored. In variance-based approaches, the uncertainty of a variable is represented by the variance of its associated probability distribution. The GSA consists in propagating the input uncertainties through the model obtaining a probabilistic estimate of the predicted shoreline, and decomposing the model output variance into several contributions, each one related to an input parameter. These contributions are used to estimate a measure of the model results sensitivity known as *first-order Sobol' index* (S_i), defined as:

$$S_i = \frac{Var\left(E(Y|X_i)\right)}{Var\,(Y)} \qquad (10)$$

where E is the expectation operator, Y is the modelled shoreline, and X_i represents the i-th uncertain variable. It should be noted that S_i only expresses the primary impact of the variable X_i on the model results uncertainty, and higher-order Sobol' indices $S_{i\ldots j}$, representing the combined effects of the independent variables $X_i \ldots X_j$, could be evaluated.

It is worth noticing that during periods when the model results are affected by a large variance, the *Si* variations are expected to be small compared to those observed in periods with smaller variance. This effect owes to the nature of the *Si* calculation (Equation 9) that is inversely proportional to the unconditional model variance. For the present study, we focus on the time varying relative impact of the uncertainty associated to SLR rate, DoC and the cross-shore module free parameters (*c, b* and Φ) on the resulting modelled shoreline (Y). The effects of SLR induced uncertainties on model results could be analysed by observing the *Si* of the ratio $SLR_{rate}/\tan\beta$. However, due to the different nature of their respective uncertainties, we address the relative impacts of SLR rate and DoC separately. An underlying assumption of the GSA is that

the input variables are statistically independent (Saltelli et al., 2008). The nature of the LX-Shore cross-shore module is such that its uncertain input parameters (*b,c, Φ*) are correlated one to the other. To account for this dependence in the computation of the S_i, we rely on the sampling-based algorithm by Li and Mahadevan (2016). When performing a GSA, one consequence of using (even slightly) correlated variables is that part of the S_i of a particular variable will also contribute to the S_i of other correlated variables, and the will be accounted multiple times. Hence, while variance decomposition performed using independent variables results in a sum of S_is ≤1, the sum of the S_is may exceed 1 when using correlated variables. Here, our goal is to conduct a 'Factors' Prioritisation' (as defined by Saltelli et al. 2008), i.e. identifying the factor that one should fix to minimize output uncertainty. With or without correlated inputs, the first-order Sobol' indices can still be considered as a valid indicator of which variable (if fixed) will mostly reduce the variance of the output as underlined for instance by Da Veiga et al. (2009). The procedure holds as follows: (a) associate a probability distribution to each uncertain input variable (SLR rate, DoC, *c, b* and *Φ*) while accounting for the dependence between the model free parameters; (b) propagate the latter distributions through the model by means of Monte-Carlo-based procedure generating a distribution of modelled shorelines; and (c) compute the S_i time series for each input variable. Figure 4 illustrates the generic and case specific methodology developed in the present work. The following section describes the design of the site-specific input probability distributions used in the present study.

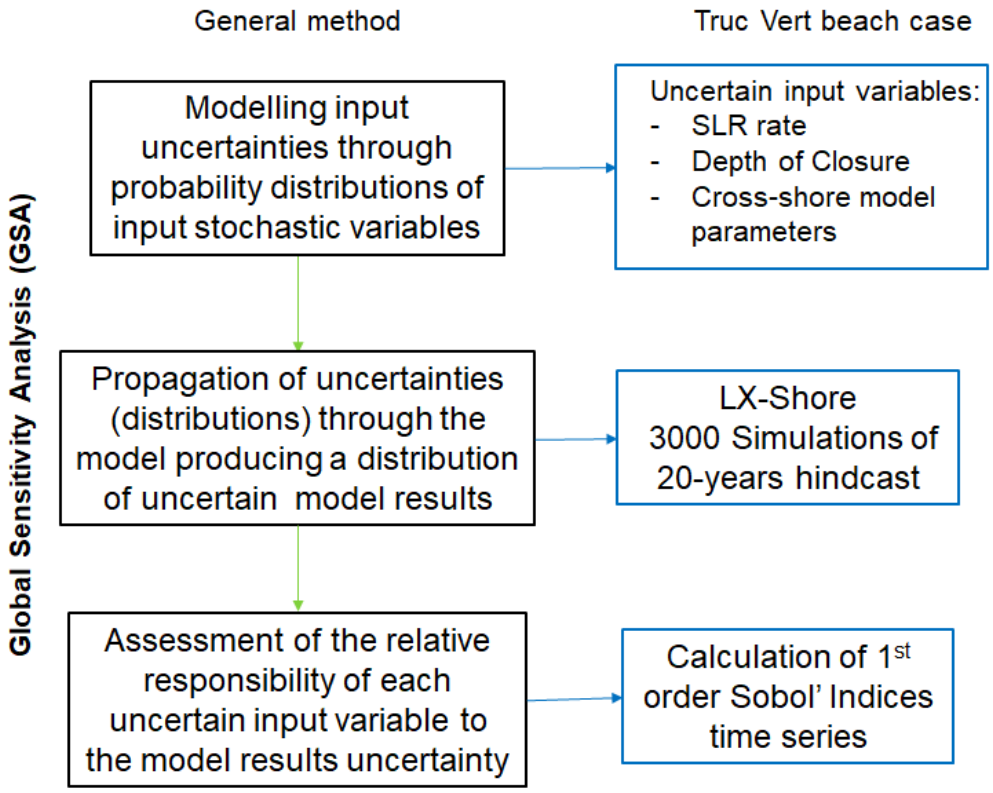

Figure 4 Schematic representation of the method developed herein

3. INPUT PROBABILITY DISTRIBUTIONS

3.1 Depth of Closure

Assuming the Bruun rule, the uncertainties associated to the impact of SLR on the shoreline are mostly due to the definition of the equivalent slope used in the formula. The dune crest level is known to have been quite stable over the past 20 years at the Truc Vert because it is part of the mechanically reprofiled dune in the 70s. Hence, the DoC primarily depends on the wave climate. The most common approach relating DoC to the yearly wave climate is using the Hallermeier (1978) formula. Therefore, we calculated the DoC over several portions of the wave climate using a 1-year moving window at a 30-day step. The resulting population of DoC is well fitted by a Gaussian

probability density curve with a mean value μ_{DoC} = 14.28m, and a standard deviation σ_{DoC} = 1.05m (Figure 5a).

3.2 Mean sea-level changes

The uncertainties affecting the reconstructed mean sea-level change account for measurement errors affecting mean sea level in the Bay of Biscay and local vertical ground motions in Lèges-Cap-Ferret. These uncertainties follow Normal distributions due to the methods used in both cases (Rohmer & Le Cozannet, 2019; Santamaría-Gómez et al., 2017), as usually assumed in reconstructions of past sea-level change (Meyssignac, Becker, Llovel & Cazenave, 2012). Residual uncertainties that cannot be quantified include the possibility that Truc Vert beach is not affected by the same subsidence rate as the Lèges Cap-Ferret GPS station, as they are separated by 8 km. Hence, over the period 1998-2018 the relative SLR rate is approximately constant, and follows a Normal probability distribution with a mean value $\mu_{SLRrate}$ = 3.31mm/year and $\sigma_{SLRrate}$ = 0.67mm/year standard deviation (Figure 5b).

3.3 Model free parameters

As numerical models are by definition an approximation of the reality, they are affected by uncertainty. LX-Shore cross-shore module has an empirical nature and requires the calibration of 3 model free parameters (*c, b* and Φ). The main source of uncertainty in the calibration process lies in the criteria used to assess the optimal combination of model free parameters. We optimized the parameters by minimizing the RMSE (root-mean-square error) between the modelled and the observed shoreline positions over

the period 2011-2018 using the Simulated Annealing algorithm (Bertsimas & Tsitsiklis, 1993). Shoreline data estimated from surveys prior to 2011 were not included in the calibration process due to the scarce confidence associated with the limited longshore coverage of the surveys (see Section 2.2.1). The uncertainties related to the quality and limited amount of observations makes reasonable to think that other combinations of *c, b* and *Φ* producing a RMSE higher than the optimal over the period 2011-2018 may perform better over the actual simulated period. For this reason, we accepted all combinations of parameters producing a RMSE lower than 10m during the iterations of the Simulated Annealing, in comparison to the minimum RMSE of 7.3m obtained using the optimised parameters over the 2011-2018 period. The RMSE limit of 10m was selected based on complementary calibration tests, which showed that optimizing the model parameters over shorter time window (3-year sliding window) between 2011 and 2018 and validating the model over the whole period 2011-2018, produced RMSE ranging between 9.3m and 13m. During the calibration procedure the LX-Shore SLR module was activated, so that the effect of SLR is explicitly expressed and segregated from the long-term parameter *b*. This procedure resulted in a population of quasi-randomly generated parameter combinations to which we fitted an empirical trivariate probability distribution using a multivariate Gaussian Kernel density estimation (Silverman, 1998; Figure 5c-e). The result of this procedure led to the possible ranges of *c, b* and *Φ* reported in Table 1, which are in line with the ones obtained in Splinter et al. (2014).

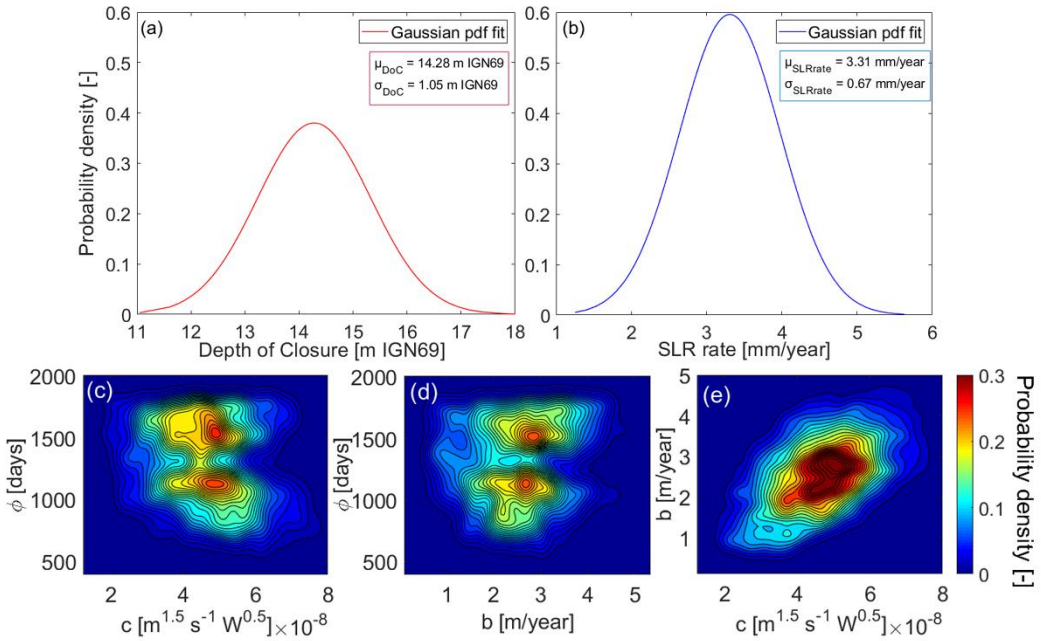

Figure 5 Probability density functions of: (a) DoC; (b) SLR rate; (c), (d) and (e) (c,Φ), (b,Φ) and (c,b) cross-shore module parameters respectively

Table 1 Best fit parameters from Simulated Annealing, variation range of the cross-shore model free parameters used in the Simulated Annealing process and in the probability distribution

Model parameter	Optimised value	Distribution range	Simulated annealing range
c **[$m^{1.5}$ s^{-1} $W^{0.5}$]**	4.5217 x10^{-8}	[1.3586; 7.7691] x10^{-8}	[0.5; 10]x10^{-8}
b **[m/year]**	2.7479	[0.2158; 4.9678]	[-6; 6]
Φ **[days]**	1638	[474; 1988]	[400; 2000]

3.4 Shoreline evolution

The distribution of modelled shoreline over the past 20 years (1998-2018) is produced by simulating the Truc Vert shoreline evolution for 3000 different combinations of the uncertain input parameters SLR rate, DoC, and (*c, b, Φ*). We generated the combinations of input parameters sampling 3000 values from their respective probability functions. Model outputs were stored at intervals of 7-days (*Dt*) over the simulated period to build the shoreline position time series. To compare the 3000

modelled shorelines, a position at a certain reference time (t_0) had to be defined. The starting date of the calibration period (5th January 2011) was chosen both to fit with observations during the calibration procedure and because uncertainties in the model results increase towards the past, where shoreline measurements are less reliable or not available (Figure 6b). Shoreline change computed with all 3000 combinations of uncertain parameters show similar behaviour with only notable differences in terms of long-term trend, and amplitude in seasonal and interannual variability (Figure 6b,c). Results show a 4-year accretion phase from 2001 to 2005 in response to a series of low-energy winters (Figure 6a), which is consistent with the observed trend at Porsmilin beach in Brittany, exposed to a similar wave climate as Truc Vert (Dodet et al., 2019). In contrast, large erosion is systematically modelled during the outstanding high-energy winter of 2013-2014. Model results are also in line with the ranges of possible shoreline positions estimated from data prior to 2011, which was not used for the calibration, but are still believed to provide a realistic indication on shoreline variability.

4. RESULTS

4.1 Global Sensitivity Analysis

The reference position at the reference time t_0 represents the point from which all modelled shorelines are projected (backwards and/or forward) in time. Therefore, there is no uncertainty (variance) of model results at t_0, and the selection of t_0 affects the evolution of the results variance over the simulated period and the corresponding Sobol' indices. The following analysis of the results is carried out using firstly the observed position at the calibration starting date as reference (t_0) for the modelled

shoreline time series (Figure 6b), such that the variance equals 0 at the beginning of the 2011 year (Figure 6c).

The *Si* time series corresponding to each uncertain input variable are shown in Figure 6d-h. The uncertainties in the 20-year shoreline hindcast are dominated by the variations of the cross-shore model free parameters (*c*, *b* and *Φ*). For the parameters *b*, *c* and *Φ* (Figure 6d-f), *Si* evolves more or less gradually with some seasonal variability during the farther past period (1998-2006) when the variance of the model results is relatively large (Figure 6c). Subsequently (2006-2018) much larger seasonal and interannual variabilities are observed, associated with smaller model variance, suggesting that model sensitivity strongly depends on wave conditions. In contrast, the *Si* curves of SLR rate and DoC remain roughly constant below 1% during the entire simulated period ($Si_{SLRrate} \in [0; 0.1]$; $Si_{DoC} \in [0.001;0.1]$) implying that on these timescales shoreline change is not sensitive to SLR. Such low impact of SLR on the model uncertainty was expected: it is due to the limited uncertainty associated with both DoC and SLR rates relative to the other variables during the analysed period. This becomes evident when comparing the mean and 99th percentiles of long-term SLR-induced erosion (2.7 m, and 3.8 m) with the effects of *b* (51.3 m, and 88.3 m) over the 20-year simulated period.

We observe that during 1998-2006 the variation of parameter *b* is responsible for most of the variance in modelled shoreline, with *Si* regularly increasing towards the past from 61% to 94%, and a notable step during the 2000-2001 high-energy winter. The regularity of the *b*'s trend in this period is due to its linear nature (in the model, *b* represents the long-term shoreline trend, see Equation 1, and is not dependent on wave conditions). Over this 1998-2006 period, the sensitivity of the model results to

parameter *c* also slightly increases (towards the past) with substantial seasonal variations, with *Si* maximised at 63% during the 2000-2001 high-energy winter. From 2006 onwards, when model variance is lower, the model sensitivity to *c* shows large inter- and intra-annual variability exceeding 90% during the high-energy winters (2013-2014 and 2015-2016) and lowering to approximately 5% during milder conditions between some winters. Over the same period, *b*'s *Si* shows a somewhat mirrored behaviour to *c*'s *Si*. The influence of beach memory parameter Φ on the results' uncertainties gradually increases from 10% in 1998 to 52% in 2006, and oscillates between 10% and 82% afterwards, and is sometimes in phase or out-of-phase of *b* and *c* *Si*s. In Table 2 we provide the average *Si* values for *c*, *b*, and Φ over the periods from January 1998 to December 2005, from January 2006 to December 2017 and the outstanding winter December 2013 to March 2014 (as an example of short term period).

To examine the influence of t_0 on the time evolution of the Sobol' indices, Figure 7a-c show *Si* time series for the full spectrum of possible reference times t_0 (for which the modelled shoreline equals 0) within the simulated period, for *b*, *c* and Φ. On these plots, a diagonal intersecting the horizontal axis (Dt=0) at a certain t_0 represents the time series of *Si*s computed observing the results in reference to t_0. Consequently, a horizontal section of the plots in Figures 7a-c (Dt = constant) represents the time series of *Si*s calculated on progressive variations of the model variance (over a time Dt) rather than the total variance. Results show that the sensitivity of the modelled shoreline to *c* (Figure 7a) increases in the short-term (see the horizontal sections with Dt approaching 0), and both seasonal and interannual variability are striking along the diagonals. The variation of *b*'s *Si* (Figure 7b) appears once again mirrored in respect to *c*'s *Si*, providing weak contribution to the uncertainties in the short term and growing

(backwards and forward) in the long-term, showing that the uncertainties associated to *b* become dominant only on the long-term for each given t_0. Figure 7c shows that *Φ*'s *Si* is mostly low with consistent seasonal variability, and that it only becomes dominant when *b* and *c* are both small. All plots show evident break-lines in *Si*, corresponding to 2000-2001, 2006-2007 and 2013-2014 and 2015-2016 high-energy winters, highlighting the importance of outstanding winters on modulating model sensitivity to the different free parameters.

Figure 8 shows the time series of progressive *Si*, calculated on the variation of modelled shoreline (dY) at each output time step *Dt* (i.e. horizontal section at *Dt* = 1 week in Figure 7a-c), to disregard the cumulative effect of the variance over time. It is observed that parameter *c* controls the response rate of the shoreline to the incident wave power (*P*, see Equations 1 and 2), driving shoreline changes at the time scales of storms (days). This illustrates how the variability of the *c* parameter over a time *Dt* is responsible for almost the entire model variance, although we also observe occasional drops in *c*'s *Si* corresponding to low-energy periods following high-energy events (Figure 6a). On this one-week time scale, the effect of the linear term *b* is negligible, and the variations of its *Si* is only related to the effect of the two other uncertain parameters (*c* and *Φ*). This is better observed in Figure 9, which shows a 90 days average of the relative *Si*s between 2013 and 2014.

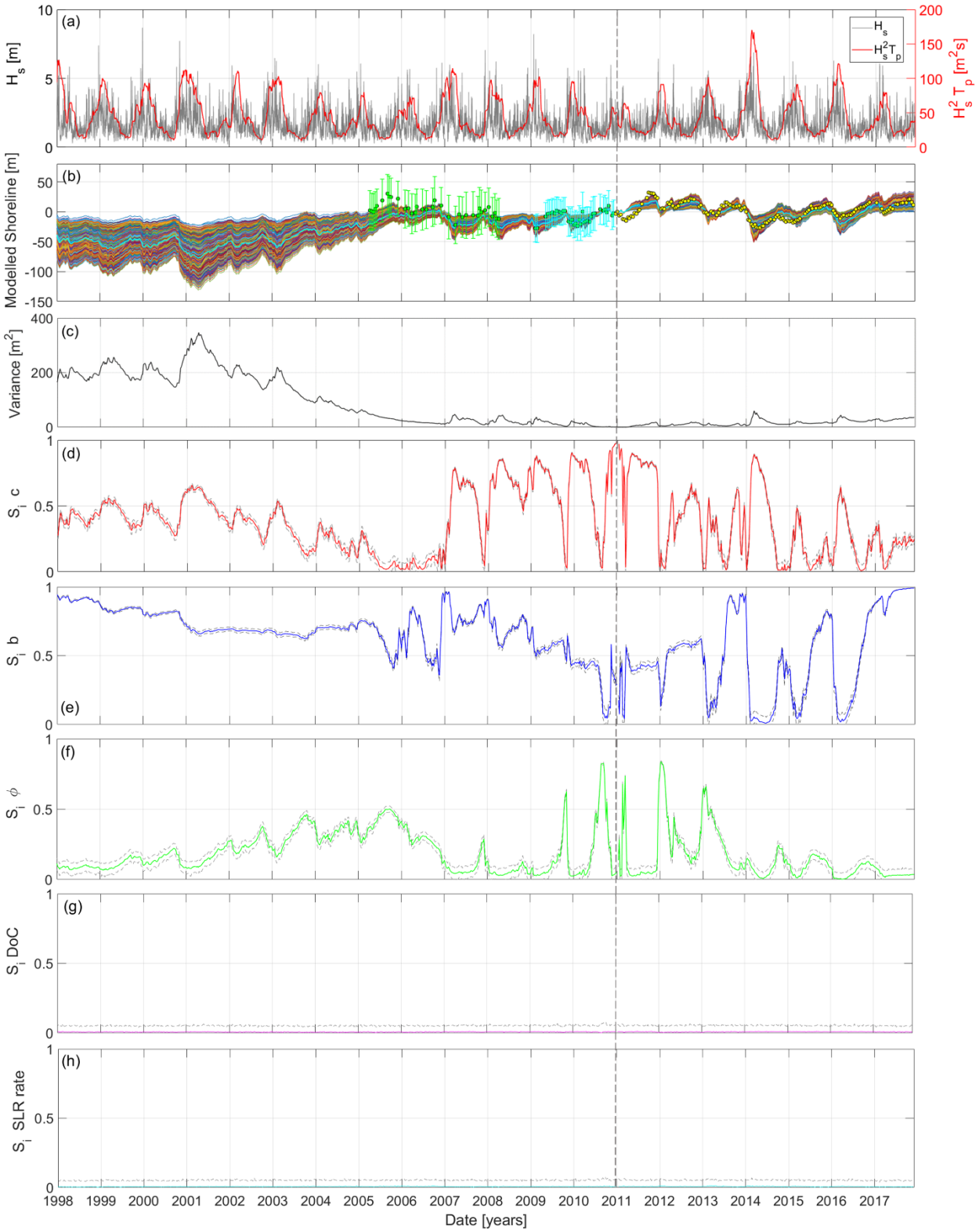

Figure 6 (a) Simulated offshore wave conditions synthetized in the average value H^2_{so}/T_p; (b) Envelope of 3000 simulated shoreline over the period 1998-2018 (coloured lines), and observed average shoreline positions between 2005 and 2017 (green before 2011 and yellow dots after 2011) with bars indicating the estimated

maximum possible range of variability due to longshore variability of the shoreline, corrected to account for limited size of the survey coverage (±28m in the period 2005-2008, green bars, and ±18m in the period 2008-2011, cyan lines); (c) model variance time series; (d) to (h) 1st order Sobol' index time series for the uncertain input variables with 3%-97% confidence interval derived from a bootstrap-based approach with 200 bootstraps (grey dash lines). The vertical dash line indicates the t_0

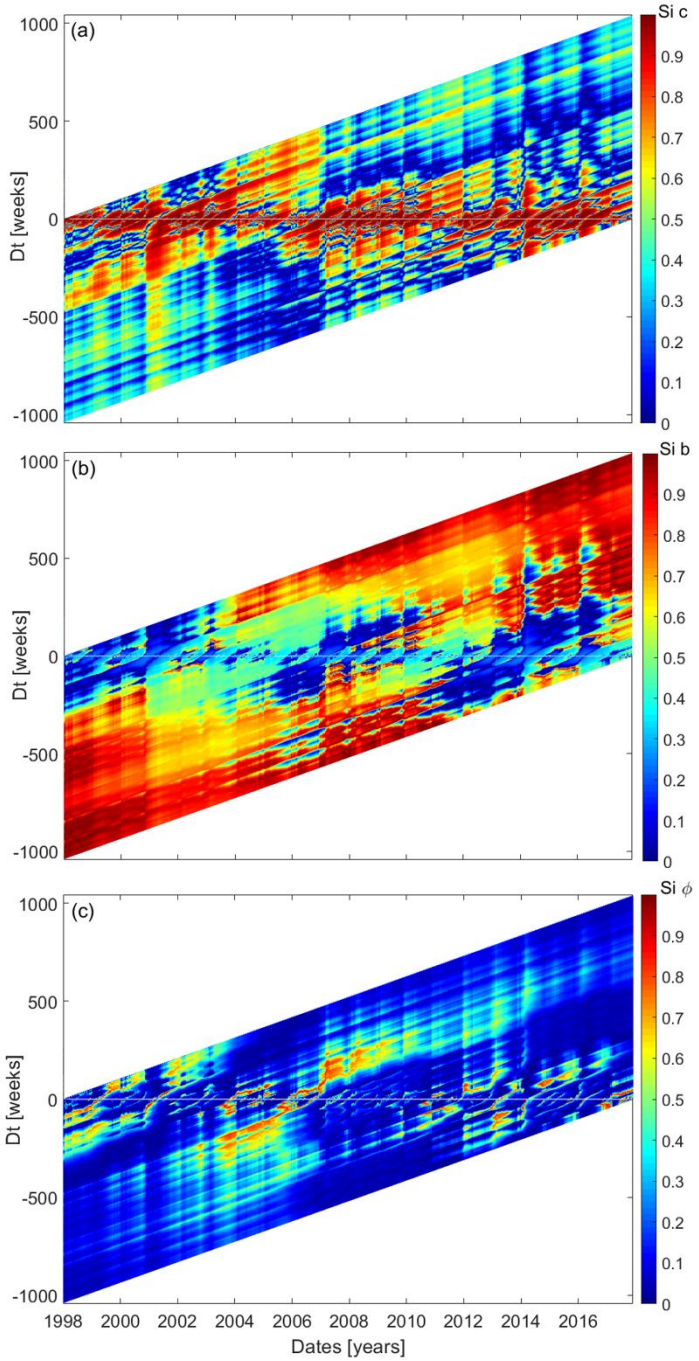

Figure 7 Full spectrum of 1st order Sobol' indices time series calculated for (a) *c*; (b) *b;* and (c) *Φ* parameters, where diagonals represent time series corresponding to each possible reference starting point

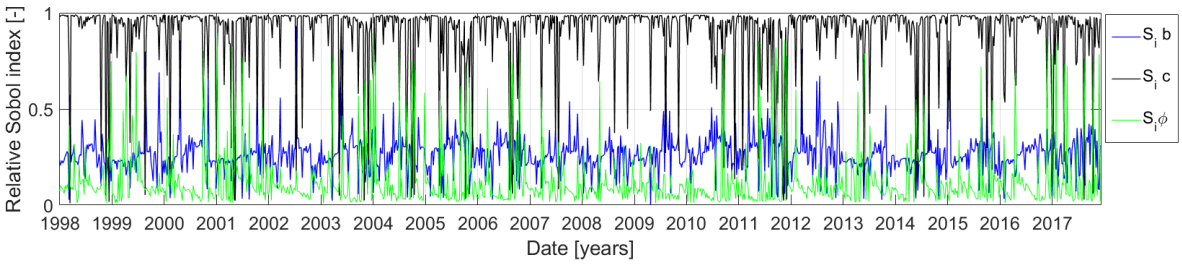

Figure 8 Progressive (Dt = 1 week) 1st order Sobol' index time series for *c*, *b,* and *Φ*, corresponding to the horizontal section for Dt=1 week of the plots showed in Figure 7a, 7b and 7c respectively

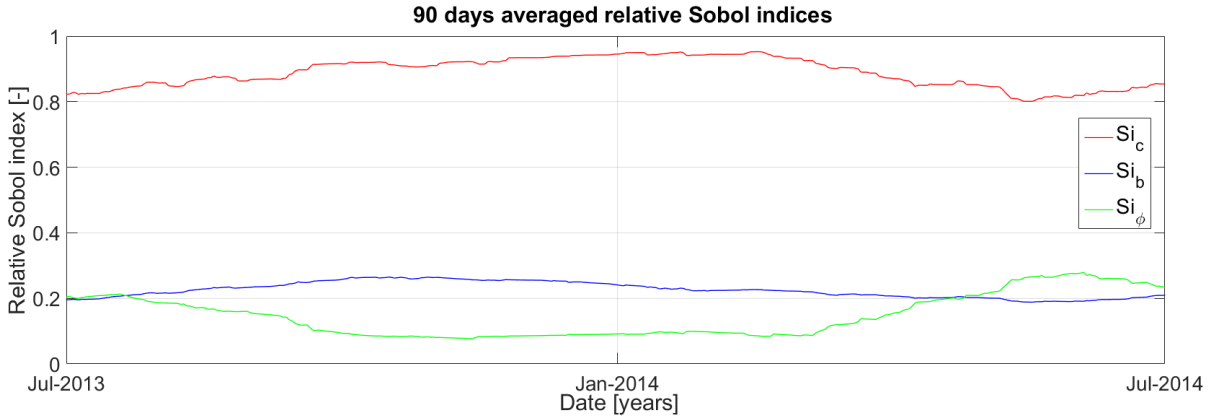

Figure 9 Time series of 90 days average relative Sovol' indices, over the period 2013-2014 forc,b and Φ.

Table 2 Mean first-order Sobol' indices for *c*, *b* and *Φ*, and mean model variance over selected periods of simulated.

Period	Mean S_i *c* [-]	Mean S_i *b* [-]	Mean S_i *Φ* [-]	Mean Model Variance [m^2]
1998- 2005	0.35	0.74	0.23	165.14
2006-2017	0.42	0.54	0.15	16.57
2013-2014	0.53	0.29	0.10	24.73

5. DISCUSSION AND CONCLUSIONS

5.1 Sea-level rise

The GSA performed on the 20-year shoreline hindcast at Truc Vert beach indicates that the uncertainties of shoreline evolutions are primarily controlled by the

uncertainties of the free parameters of the wave-driven (cross-shore) model. This means that the contribution of the uncertainties associated to the past SLR rate and DoC, which influence SLR-driven chronic erosion, are negligible comparing to the uncertainties affecting the wave-driven model parameters on these timescales. This is not surprising given that SLR acts on long timescales and that uncertainties of SLR estimates over the period of interest. For instance, previous work showed that uncertainties of future shoreline change, as sea level rises, are primarily related to interannual variability of storm events during the next decades (Le Cozannet et al., 2016). The effects of SLR uncertainties may only emerge from natural shoreline change variability during the second half of the 21st century (Le Cozannet et al., 2016), together with uncertainties related to future emission gas scenario and validity of SLR-driven erosion model (Le Cozannet et al., 2019). It is however important to note that current sea-level projections may underestimate future SLR as they may slightly underestimate future ice-sheets melting (Jevrejeva et al., 2019), thus reducing the timescales of emergence of widespread SLR-induced sandy shoreline retreat. Therefore, a relevant research avenue is to account for wave-driven shoreline uncertainties that were addressed here together with updated SLR projections (Toimil et al., 2020). Building on state-of-the-art RCMs of shoreline change such as LX-Shore and others (e.g. Antolínez, Méndez, Anderson, Ruggiero, & Kaminsky, 2019; Robinet et al., 2018; Vitousek et al., 2017b) will also allow addressing the natural variability of uncertainty contributions, as the respective contributions of the processes driving shoreline change (e.g. longshore and cross-shore processes, sediment supply from nearby rivers) and their related uncertainties are essentially site specific.

5.2 Wave-driven model uncertainties and implications for model calibration and shoreline projections

Our results show that the respective contributions of the wave-driven model free parameters to shoreline change uncertainties are strongly variable in time. The response rate parameter *c* which represents a measure of the rate at which the shoreline responds to incident wave conditions and the beach memory parameter Φ reflecting the impact of antecedent wave conditions (Splinter et al., 2014) both show a strong and mirrored seasonality of their impact on the modelled shoreline. The linear parameter *b*, which accounts for the effects of long-term processes that are not included in the model, shows complex patterns. In fact, despite the simplicity of *b*'s role in the governing equations (Equation 1) and the consequent long-term effects of its variability on the model variance, its impact relative to the other uncertain variables (*Si*) is not obvious. The parameter *b* dominates the shoreline variance during extended low-energy periods, and its *Si* dramatically drops during high-energy winters. This large time variation of the free parameter uncertainties explains why the calibration period is critical to shoreline model skill when performing shoreline hindcast (Splinter et al., 2013). Given that *b* is expected to account for other processes that are not taken into account in the model, the growing sensitivity of the model results on *b* towards the past (and future) also suggests that improving wave-driven shoreline change models may significantly reduce the uncertainties affecting the modelled shoreline positions at the timescales of years to decades. Such improvement would limit and delay the long-term effects of *b* overwhelming the effects of other variables contributing to the model uncertainties, allowing to address the model sensitivity to other processes at large time scales. A better understanding of short-term processes would reduce uncertainties on the *c* parameter, significantly reducing the uncertainties at seasonal scale. The

generally low sensitivity of modelled shoreline to Φ, in spite of its large variability (Figure 5c-d), is consistent with the findings from Splinter et al. (2014) for high-energy beaches and large values of Φ. A complementary analysis of Φ's S_i evolution, where we only addressed the model sensitivity using $\Phi < 1000$ days, showed only an increase in model sensitivity to Φ during extended low-energy periods (i.e. 2001-2006) with no other substantial change comparing to Figure 6d-f, once again supporting Splinter et al. (2014) results.

Our result show that the intra-annual and interannual distribution of wave energy is critical for the model free parameter uncertainties, which also explain why even subtle changes in wave energy distribution can dramatically change the mode of shoreline response as observed by Splinter et al. (2017). To further investigate the role of interannual wave energy variability on parameter uncertainties we simulated two idealized cases preserving the model setup used for the real case and using the same distributions of uncertain model inputs, but using different distribution of wave energy. In the case of shoreline change forced by a seasonal wave climate extracted from the real wave time series (including winter 1998-1999) in the absence of interannual energy variability (Figure 10a-c), the *Si*s are quasi steady with only little seasonal variability, once again with mirrored behaviours of *b*'s and *c*'s *Si*. In addition, consistently with the above discussion, Figure 10b,c shows that an increase (decrease) in offshore wave energy results in higher (lower) model sensitivity to *c*, and vice versa to *b*. A second idealized case was ran to address the effects of interannual distribution of wave energy alternating high-energy and low-energy winters every four years (Figure 11). In this case, the winter 2002-2003 was extracted from the real wave climate to represent a low-energy winter, and the same conditions were amplified by 40% in significant wave height and 20% in peak wave period to generate a high-energy

winter. In addition to the effects observed in the previous idealized case, large interannual variations of the *Si*s are observed. We also observe the cumulative effect of *b,* which gradually overwhelms those of *c* on the long-term.

The dependence of the model sensitivity to the wave energy variability also has implications for shoreline change projections in the frame of climate change, which are regionally variable. In some regions the wave climate is expected to be only slightly affected by climate change, such as in the Bay of Biscay where Truc Vert beach is located (Charles, Idier, Delecluse, Déqué, & Le Cozannet, 2012; Perez, Menendez, Camus, Mendez & Losada, 2015). In these regions, efforts to predict future shoreline change on open coasts should be put into improving wave-driven models and in particular better accounting for other long-term processes that are implicitly accounted through *b*. In contrast, in some regions of the world, climate change will have a profound impact on wave climate and extremes and, in turn, on the uncertainties associated to the model free parameters related to the wave energy (e.g. *c* and *Φ* in the LX-Shore model), introducing an additional component of uncertainty to the projection.

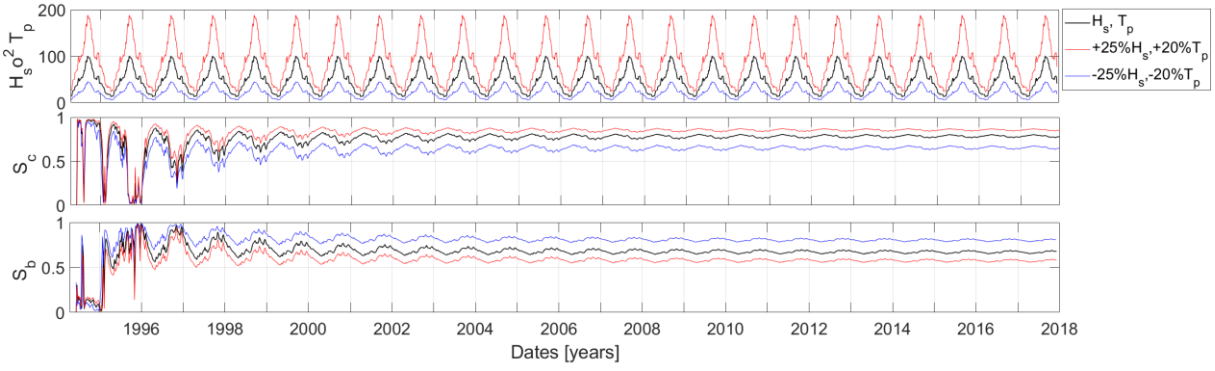

Figure 10 : Idealized seasonal wave climate, with increased (red curves) and decreased (blue curves) intensity. (a) Simulated seasonal wave conditions; (b) and (c) Sobol' indices of the free parameters *c* and *b* respectively

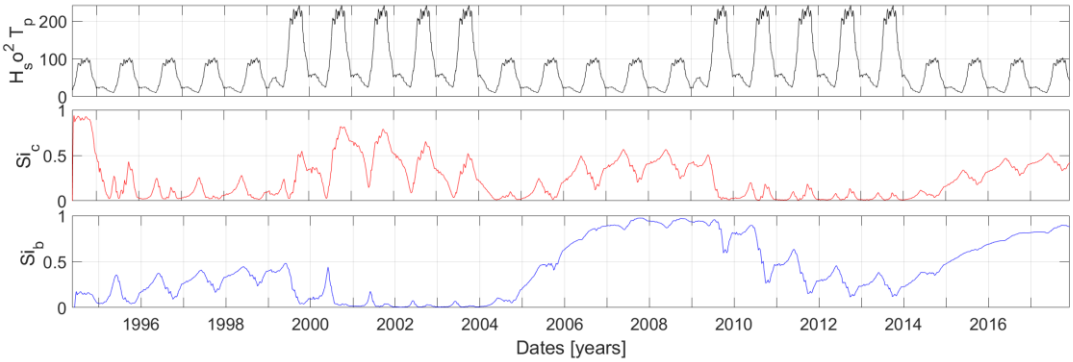

Figure 11 Idealized alternate low-energy and high-energy winters every 4 years. (a) Simulated seasonal wave conditions; (b) and (c) Sobol' indices of the free parameters *c* and *b* respectively

5.3 Assumptions and limitations

The LX-Shore cross-shore module used herein is based on disequilibrium conditions determined by the recent history of dimensionless fall velocity at the site (Equation 4) i.e. on antecedent wave conditions, regardless of the previous shoreline position. In contrast, other existing equilibrium models assume that the disequilibrium is determined by current shoreline position (Yates et al., 2009). Hence, although these two models show similar skill and shoreline change patterns at Truc Vert (Castelle et al., 2014), there is an additional source of uncertainty related to the choice of the approach for defining the disequilibrium state. The application of the method proposed in this paper using a different disequilibrium approach would allow assessing the results sensitivity to the choice of the model, similarly to the analysis carried out by Le Cozannet et al. (2019) and Montaño et al. (2020). However, this belongs to future research.

Here, we only addressed the first-order order Sobol' indices for the uncertain inputs, and combined effects of variables uncertainties (higher-order Sobol' indices as well as

total effect indices) were not evaluated. An assessment of higher-order effects would require a larger number of model results to calculate the conditional variances. Estimating the minimum amount of simulations required for a reliable evaluation of 2nd order Sobol' indices would need a convergence analysis, consistently with the analysis performed by Benaichouche and Rohmer (2016) on several test cases, which may result in a prohibitive number of simulations. The first-order Sobol' index is still an informed choice to rank the importance of correlated model inputs, when defined by using average local variances instead of specifically located variances (Li & Mahadevan, 2016; Saltelli & Tarantola, 2002). However, addressing higher-order Sobol' indices may confirm the low-impact character of certain variables (such as Φ) within a factor fixing setting as described in Saltelli et al. (2008). The possibility to address second-order Sobol' indices can be explored in future research works. A second limitation of the present work is that the results reported here apply to a given high-energy open beach, which is known both to be cross-shore transport dominated and to respond predominantly at the seasonal scale (Splinter et al., 2014). Other beaches, such as Narrabeen (SE Australia) may respond at the scale of single storms and be more sensitive to variations of the model parameter Φ (Splinter et al., 2014), resulting in very different probability distributions of model free parameters or be affected by other processes such as longshore sand transport (Harley, Turner, Short, & Ranasinghe, 2011). Further research work is required to understand the uncertainties on different types of coastal setting.

5.4 Concluding remarks

A Global Sensitivity Analysis was performed on a 20-year shoreline hindcast at Truc Vert beach. We computed the first-order order Sobol' index time series for all the identified uncertain input variables, namely sea-level rise rate, closure depth and wave-driven model free parameters (c, b and Φ). We found that, on this 20-year time span, shoreline change uncertainties are primarily the result of uncertainties on the wave-driven free parameters, with the influence of SLR and DoC uncertainties being negligible. However, the respective contributions of the uncertainties related to each model free parameter are strongly variable in time, in response to the intra-annual and interannual distribution of incident wave energy. This means that such shoreline change models need to be trained with long-term time series comprising a substantial number of representative high-energy and low-energy storm seasons. In addition, our results have strong implications from the perspective of shoreline projections in the frame of climate change. In some regions of the world, climate change may largely affect wave climate and extremes, which in turn challenges the validity of calibration parameters in the future and, ultimately, the validity of projections. The approach developed herein is applicable at other sites worldwide using any fast running shoreline model. Therefore, application of this methodology to coastlines controlled by different driving processes is encouraged to address the genericity of our results.

6. REFERENCES

Allenbach, K., Garonna, I., Herold, C., Monioudi, I., Giuliani, G., Lehmann, A., & Velegrakis, A. F. (2015). Black Sea beaches vulnerability to sea level rise. *Environmental Science & Policy, 46*, 95-109. doi:10.1016/j.envsci.2014.07.014

Antolínez, J. A. A., Méndez, F. J., Anderson, D., Ruggiero, P., & Kaminsky, G. M. (2019). Predicting climate driven coastlines with a simple and efficient multi-scale model. *Journal of Geophysical Research: Earth Surface, 124*, 1596-1624.doi:10.1029/2018JF004790

Benaichouche, A., & Rohmer, J. (2016). *Sobol' indices and variance reduction diagram estimation from samples used for uncertainty propagation.* In VIII International Conference on Sensitivity Analysis of Model Output. Tampon, Réunion. hal-brgm.archives-ouvertes.fr/hal-01338344

Bertsimas, D., & Tsitsiklis, J. (1993). Simulated annealing. *Statistical Science, 8*(1), 10–15. doi:10.1214/ss/1177011077

Bird, E. C. F. (1985). *Coastline Changes*. A Global Review. New York, NY: John Wiley & Sons Inc. doi:10.1002/gj.3350210215

Bruun, P. (1962). Sea-level rise as a cause of shore erosion. *Journal of the Waterways and Harbors Division, 88* (1), 117–132.

Bruun P.(1988). The Bruun Rule of Erosion by sea-level rise: A discussion on large-scale two- and three- dimentional usages. *Journal of Coastal Research, 4*(4), 627-648.

Casas-Prat, M., McInnes, K. L., Hemer, M. A., & Sierra, J. P. (2016). Future wave-driven coastal along the Catalan coast (NW Mediterranean). *Regional Environmental Change, 16*(6), 1739-1750. doi:10.1007/s10113-015-0923-x

Castelle, B., Bonneton, P., Dupuis, H., & Sénéchal, N. (2007). Double bar beach dynamics on high-energy meso-macrotidal French Aquitanian coast: a review. *Marine Geology, 245* (1-4), 141-159. doi:10.1016/j.margeo.2007.06.001

Castelle, B., Marieu, V., Bujan, S., Ferreira, S., Parisot, J., Capo, S., Sénéchal, N., & Chouzenoux, T. (2014). Equilibrium shoreline modelling of high energy meso-macrotidal multiple barred beach. *Marine Geology*, *347*, 85-94. doi:10.1016/j.margeo.2013.11.003

Castelle, B., Marieu, V., Bujan, S., Splinter, K. D., Robinet, A., Sénéchal, N., & Ferreira, S. (2015). Impact of the winter 2013–2014 series of severe Western Europe storms on a double-barred sandy coast: beach and dune erosion and megacusp embayments. *Geomorphology, 238*, 135-148. doi:10.1016/j.geomorph.2015.03.006

Castelle, B., Bujan, S., Ferreira, S., & Dodet, G. (2017). Foredune morphological changes and beach recovery from the extreme 2013/2014 winter at a high-energy sandy coast. *Marine Geology, 385*, 41-55. doi:10.1016/j.margeo.2016.12.006

Castelle, B., Dodet, G., Masselink, & G., Scott, T. (2017). A new climate index controlling winter wave activity along the Atlantic coast of Europe: The West Europe Pressure Anomaly. *Geophysical Research Letters, 44* (3), 1384-1392. doi :10.1002/2016GL072379

Castelle, B., Guillot, B., Marieu, V., Chaumillon, E., Hanquiez, V., Bujan, S., & Poppeschi, C. (2018). Spatial and temporal patterns of shoreline change of a 280-km high-energy disrupted sandy coast from 1950 to 2014: SW France. *Estuarine, Coastal, and Shelf Science, 200*, 212-223. doi:10.1016/j.ecss.2017.11.005

Castelle, B., Dodet, G., Masselink, G., & Scott, T. (2018). Increased winter-mean wave height, variability and periodicity in the North-East Atlantic over 1949-2017. *Geophysical Research Letters, 45*(8), 3586-3596. doi:10.1002/2017GL076884

Charles, E., Idier, D., Delecluse, P., Déqué, M., & Le Cozannet, G. (2012). Climate change impact on waves in the Bay of Biscay, France. *Ocean Dynamics, 62*(6),831-848. doi:10.1007/s10236-012-0534-8

Charles, E., Idier, D., Thiébot, J., Le Cozannet, G., Pedreros, R., Ardhuin, F., & Planton, S. (2012). Present wave climate in the Bay of Biscay: spatiotemporal variability and trends from 1958 to 2001. *Journal of Climate, 25*, 2020-2039. doi:10.1175/JCLI-D-11-00086.1

Cooper, J. A. G., & Pilkey, O. H. (2004). Sea-level rise and shoreline retreat: time to abandon the Bruun Rule. *Global Planet Change*, *43*(3-4), 157-171. doi:10.1016/j.gloplacha.2004.07.001

Da Veiga, S., Wahl, F., & Gamboa, F. (2009). Local polynomial estimation for sensitivity analysis on models with correlated inputs. *Technometrics*, 51(4), 452-463. doi:10.1198/TECH.2009.08124

Davidson, M. A., Splinter, K. D., & Turner, I. L. (2013). A simple equilibrium model for predicting shoreline change. *Coastal Engineering, 73*, 191-202. doi:10.1016/j.coastaleng.2012.11.002

Dodet, G., Castelle, B., Masselink, G., Scott, T., Davidson, M., Floc'h, F., … & Suanez, S. (2019). Beach recovery from extreme storm activity during the 2013–14 winter along the Atlantic coast of Europe. *Earth Surface Processes and Landforms*, *44*(1), 393-401. doi:10.1002/esp.4500

Gallagher, E. L., MacMahan, J. H., Reniers, A., Brown, J., & Thornton, E. B. (2011). Grain size variability on a rip-channeled beach. *Marine Geology, 287*(1-4), 43–53. doi:10.1016/j.margeo.2011.06.010

Ghermandi, A., & Nunes, P. (2013). A global map of coastal recreation values: Results from a spatially explicit meta-analysis. *Ecological Economics, 86*, 1-15. doi:10.1016/j.ecolecon.2012.11.006

Hallermeier, R. J. (1978). *Uses for a calculated limit depth to beach erosion.* In: Proceedings of the 16th Coastal Engineering Conference. ASCE, New York, 1493-1512.

Hallin, C., Larson, M., & Hanson, H. (2019). Simulating beach and dune evolution at decadal to centennial scale under rising sea levels. *PLoS ONE*, *14*(4): e0215651. doi:10.1371/journal.pone.0215651

Harley, M. D., Turner, I. L., Short, A. D., & Ranasinghe, R. (2011). A re-evaluation of coastal embayment rotation: The dominance of cross-shore versus alongshore sediment transport processes, Collaroy-Narrabeen Beach, southeast Australia. *Journal of Geophysical Research: Atmosphere, 116*, F04033, doi:/10.1029/2011JF001989

Hinkel, J., Church, J.A., Gregory, J.M., Lambert, E., Le Cozannet, G., Lowe, J., ... & van de Wal, R.. (2019). Meeting user needs for sea level rise information: A decision analysis perspective. *Earth's Future*, *7*, 320-337. doi.org/10.1029/2018EF001071

Jevrejeva, S., Frederikse, T., Kopp, R. E., Le Cozannet, G., Jackson, L. P., & van de Wal, R. S. W. (2019). Probabilistic Sea Level Projections at the Coast by 2100. *Surveys in Geophysics*, 1-24. doi:10.1007/s10712-019-09550-y

Laporte-Fauret, Q., Marieu, V., Castelle, B., Michalet, R., Bujan, S., & Rosebery, D. (2019). Low-Cost UAV for High-Resolution and Large-Scale Coastal Dune Change Monitoring Using Photogrammetry. *Journal of Marine Science and Engineering, 7*(3), 63. doi:10.3390/jmse7030063

Larson, M., Hogan, L. X., & Hanson, H. (2010). Direct formula to compute wave height and angle at incipient breaking. *Journal of Waterway Port, Coastal and Ocean Engineering, 136*(2), 119–122. doi:10.1061/(ASCE)WW.1943-5460.0000030

Le Cozannet, G., Oliveros, C., Castelle, B., Garcin, M., Idier, D., Pedreros, R., & Rohmer, J. (2016). Uncertainties in sandy shorelines evolution under the Bruun rule assumption. *Frontiers of Marine Science, 3*, 49, doi:10.3389/fmars.2016.00049

Le Cozannet, G., Castelle, B., Ranasinghe, R., Wöppelmann, G., Rohmer, J., Bernon, N., … & Salas-y-Mélia, D. (2019). Quantifying uncertainties of sandy shoreline change projections as sea level rises. *Scientific Reports, 42(9).* doi:10.1038/s41598-018-37017-4

Lemos, C., Floc'h, F., Yates, M., Le Dantec, N., Marieu, V., Hamon, K., & Delacourt, C. (2018). Equilibrium modelling of the beach profile on a macrotidal embayed low tide terrace beach. *Ocean Dynamics, 68*(9), 1207-1220. doi:10.1007/s10236-018-1185-1

Li, C., & Mahadevan, S. (2016). An efficient modularized sample-based method to estimate the first-order Sobol' index. *Reliability Engineering and System Safety*, *153*, 110-121. doi:10.1016/j.ress.2016.04.012

Ludka, B. C., Guza, R. T., O'Reilly, W. C., & Yates, M. L. (2015). Field evidence of beach profile evolution toward equilibrium. *Journal of Geophysical Research: Oceans*, 120(11), 7574-7597. doi:10.1002/2015JC010893

Luijendijk, A., Hagenaars, G., Ranasinghe, R., Baart, F., Donchyts, G., & Aarninkhof, S. (2018). The State of the World's Beaches. *Scientifc Reports*, *8*, 6641. doi:10.1038/s41598-018-24630-6

Masselink, G., Castelle, B., Scott, T., Dodet, G., Suanez, S., Jackson, D., & Floc'h, F. (2016). Extreme wave activity during 2013/2014 winter and morphological impacts along the Atlantic coast of Europe. *Geophysical Research Letters*, *43*(5), 2135-2143. doi:10.1002/2015GL067492

Mentaschi, L., Vousdoukas, M.I., Pekel, J-F., Voukouvalas, E., & Feyen, L. (2018). Global long-term observations of coastal erosion and accretion. *Scientific Reports*. *8*, 12876. doi:10.1038/s41598-018-30904-w

Meyssignac, B., Becker, M., Llovel, W., & Cazenave, A. (2012). An Assessment of Two-Dimentional Past Sea Level Reconstructions Over 1950-2009 Based on Tide-gauge Data and Different Input Sea Level Grids. *Surveys in Geophysics, 33*(5), 945-972. doi:10.1007/s10712-011-9171-x

Michaud, H., Pasquet, A., Leckler, F., Baraille, R., Dalphinet, A., & Aouf, L. (2016). *Improvements of the new French coastal wave forecasting system and application to a wave-current interaction study*. SHOM & Meteo France. doi:10.13140/RG.2.2.13218.02243

Montaño, J., Coco, G., Antolínez, J. A.A., Beuzen, T., Bryan, K. R., Cagigal, L., …, & Vos, K., (2020). Blind testing of shoreline evolution models.

Neumann, B., Vafeidis, A.T., Zimmermann, J., & Nicholls, R.J. (2015). Future Coastal Population Growth and Exposure to Sea-Level Rise and Coastal Flooding—A Global Assessment. *PLoS ONE, 10*(3): e0118571. doi:10.1371/journal.pone.0118571

Parisot, J. P, Capo, S., Castelle, B., Bujan S., Moreau, J. M., Gervais, M., … & Senechal, N. (2009). Treatment of topographic and bathymetric data acquired at the Truc-Vert Beach (SW France) during the ECORS field experiment [Special issue]. *Journal of Coastal Research, 56,* Proceedings of the 10th International Coastal Symposium ICS 2009, Vol. II, 1786-1790. www.jstor.org/stable/25738097

Perez, J., Menendez, M., Camus, P., Mendez, F. J., & Losada, I. J. (2015). Statistical multi-model climate projections of surface ocean waves in Europe. *Ocean Modelling*, 96, 161-170. doi:10.1016/j.ocemod.2015.06.001

Ranasinghe, R., Callaghan, D., & Stive, M. J. F. (2012). Estimating coastal recession due to sea-level rise: Beyond the Bruun rule. *Climatic Change, 110*(3-4), 561–574. doi:10.1007/s10584-011-0107-8

Robinet, A., Castelle, B., Idier, D., Le Cozannet, G., Déqué, M., & Charles, E. (2016). Statistical modeling of interannual shoreline change driven by North Atlantic climate variability spanning 2000–2014 in the Bay of Biscay. *Geo-Marine Letters 36*(6), 479–490. doi:10.1007/s00367-016-0460-8

Robinet, A., Idier, D., Castelle, B., & Marieu, V. (2018). A reduced-complexity shoreline change model combining longshore and cross-shore processes: The LX-Shore model. *Environmental Modelling and Software, 109*, 1-16. doi:10.1016/j.envsoft.2018.08.010

Robinet, A., Castelle, B., Idier, D., Harley, M. D., Splinter, K. D. (2020, in press). Controls of local geology and cross-shore/longshore processes on embayed beach shoreline variability. *Marine Geology.* In press. doi :10.1016/j.margeo.2020.106118Rohmer, J. & Le Cozannet, G. (2019). Dominance of the mean sea level in high-percentile sea levels time evolution with respect to large-scale climate variability: a Bayesian statistical approach. *Environmental Research Letters, 14*(1). doi:10.1088/1748-9326/aaf0cd

Saltelli, A., & Tarantola, S. (2002). On the relative importance of input factors in mathematical models. *Journal of the American statistical association, 97*(459), 702-709. doi:10.1198/016214502388618447

Saltelli, A., Ratto, M., Andres T., Campolongo, F., Cariboni, J., Gatelli, D., … & Tarantola, S. (2008). *Global Sensitivity Analysis : The premier*. Jhon Wiley & sons.

Santamaría-Gómez, A., Gravelle, M., Dangendorf, S., Marcos, M., Spada, G., & Wöppelmann, G. (2017). Uncertainty of the 20th century sea-level rise due to vertical land motion errors. *Earth and Planetary Science Letters*. 473, 24-32. doi:10.1016/j.epsl.2017.05.038

Sénéchal, N., Gouriou, T., Castelle, B., Parisot, J. P., Capo, S., Bujan, S., & Howa, H. (2009). Morphodynamic response of a meso-macrotidal intermediate beach based on a long-term dataset. *Geomorphology*, *107*, 263-274. doi:10.1016/j.geomorph.2008.12.016

Silverman, B. W. (1998). *Density Estimation for Statistics and Data Analysis*. New York: Routledge. doi:10.1201/9781315140919

SHOM (2017), *Références Altimétriques Maritimes* [Maritime Altimetry References], ISBN 978-2-11-139469-8.

Sobol', I. M. (2001). Global sensitivity indices for nonlinear mathematical models and their Monte Carlo estimates. *Mathematics and Computers in Simulation*, *55*(1-3), 271-280. doi:10.1016/S0378-4754(00)00270-6

Splinter, K., Turner, I. L., & Davidson, M. A. (2013). How much data is enough? The importance of morpghological sampling interval and duration for calibration of empirical shoreline models. *Coastal Engineering, 77*, 14-27. doi:10.1016/j.coastaleng.2013.02.009

Splinter, K., Turner, I. L., Davidson, M. A., Bernard, P., Castelle, B., & Oltman-Shay, J. (2014). A generalized equilibrium model for predicting daily to interannual shoreline response. *Journal of Geophysical Research: Earth Surface, 119*(9), 1936-1958. doi:10.1002/2014JF003106

Splinter, K., Turner, I. L., Reinhardt, M., & Ruessink, G. (2017). Rapid adjustment of shoreline behaviour to changing seasonality of storms: observations and modelling at an open-coast beach. *Earth Surface Processes and Landforms, 42*(8), 1186-1194. doi:10.1002/esp.4088

Toimil, A., Losada, I. J., Camus, P., & Diaz-Simal, P. (2017). Managing coastal erosion under climate change at regional scale. *Coastal Engineering, 128*, 106-122. doi:10.1016/j.coastaleng.2017.08.004

Toimil, A., Diaz-Simal, P., Losada, I.J., & Camus, P. (2018). Estimating the risk of loss of beach recreation value under climate change. *Tourism Management, 68*, 387-400. doi:10.1016/j.tourman.2018.03.024

Toimil, A., Camus, P., Losada, I.J., Le Cozannet, G., Nicholls, R., Idier, D., & Maspataud, A. (2020). Climate Change Driven coastal erosion modelling in temperate sandy beaches methods and uncertainty treatment. *Earth Science Reviews*. Currently under review.

Vitousek, S., Barnard, P. L., & Limber, P. (2017a). Can beaches survive climate change? *Journal of geophysical research: Earth Surface*, *122*(4), 1060-1067. doi:10.1002/2017JF004308

Vitousek, S., Barnard, P. L., Limber, P., & Erikson, L., Cole, B. (2017b). A model integrating longshore and cross-shore processes for predicting long-term shoreline response to climate change. *Journal Geophysical Research: Earth surface, 122* (4), 782–806. doi:10.1002/2016JF004065

Wainwright, D. J., Ranasinghe, R., Callaghan, D. P., Woodroffe, C. D., Jongejan, R., Dougherty, A. J., … & Cowell, P. J. (2015). Moving from deterministic towards probabilistic coastal hazard and risk

assessment: development of a modelling framework and application to Narrabeen Beach, New South Wales, Australia. *Coastal Engineering, 96*, 92-99. doi:10.1016/j.coastaleng.2014.11.009

Wong, P .P., Losada, I. J., Gattuso, J. P., Hinkel, J., Khattabi, A., McInnes, K. L., … & Sallenger, A. (2014). *Coastal systems and low-lying areas*. *In: Climate Change 2014: Impacts,Adaptation, and Vulnerability. Part A: Global and Sectoral Aspects*. Contribution of working group II to the Fifth Assessment Report of the Intergovernmental Panel on Climate Change. Cambridge, United Kingdom and New York, NY, USA: Cambridge University Press, 361-409.

Wright, L. D., & Short, A. D. (1984). Morphodynamic variability of surf zones and beaches: a synthesis. *Marine Geology, 56*(1-4), 93-118. doi:10.1016/0025-3227(84)90008-2

Yates, M. L., Guza, R. T., & O'Reilly, W. C. (2009). Equilibrium shoreline response: Observations and modeling. *Journal of Geophysical Research: Oceans*, *114*(C9), C09014. doi:/10.1029/2009JC005359

Added References (Integrated in the list already)

Bruun P.(1988). The Bruun Rule of Erosion by sea-level rise: A discussion on large-scale two- and three- dimentional usages*. Journal of Coastal Research,* 4(4), 627-648*.*
Montaño, J., Coco, G., Antolínez, J. A.A., Beuzen, T., Bryan, K. R., Cagigal, L., …, & Vos, K., (2020). Blind testing of shoreline evolution models.

Da Veiga, S., Wahl, F., & Gamboa, F. (2009). Local polynomial estimation for sensitivity analysis on models with correlated inputs. *Technometrics*, 51(4), 452-463. doi:10.1198/TECH.2009.08124

Perez, J., Menendez, M., Camus, P., Mendez, F. J., & Losada, I. J. (2015). Statistical multi-model climate projections of surface ocean waves in Europe. *Ocean Modelling*, 96, 161-170. doi:10.1016/j.ocemod.2015.06.001

Ranasinghe, R. (2020). On the need for a new generation of coastal change models for the 21st century. *Sci Rep* 10, 2010. doi:10.1038/s41598-020-58376-x

Robinet, A., Castelle, B., Idier, D., Harley, M. D., Splinter, K. D. (2020, in press). Controls of local geology and cross-shore/longshore processes on embayed beach shoreline variability. *Marine Geology.* In press*.* doi:10.1016/j.margeo.2020.106118

Toimil, A., Camus, P., Losada, I.J., Le Cozannet, G., Nicholls, R., Idier, D., & Maspataud, A. (2020). Climate Change Driven coastal erosion modelling in temperate sandy beaches methods and uncertainty treatment. *Earth Science Reviews*. Currently under review.

Acknowledgments

This work is co-financed by the BRGM and Make Our Planet Great Again (MOPGA) national program. BC funded by Agence Nationale de la Recherche (ANR) grant number ANR-17-CE01-0014. This study includes the monitoring study site of Truc Vert labelled by the Service National d'Observation (SNO) Dynalit (https://www.dynalit.fr) with additional support from Observatoire Aquitaine de l'Univers (OASU) and Observatoire de la Côte Aquitaine (OCA). The authors thank the colleagues, including Stephane Bujan, Sophie Ferreira and Vincent Marieu involved in the topographic data; LOPS-Ifremer for NORGAS-UG wave data; and SONEL for sea levels and vertical land motion data.

DATA AVAILABILITY STATEMENT

Data sharing is not applicable to this article as no new data were created or analyzed in this study.

CONFLICTS OF INTEREST

The authors declare that there is no conflict of interest that could be perceived as prejudicing the impartiality of the research reported.